

Supplementary Material

Enhanced efficiency of the Sb₂Se₃ thin-film solar cell by the anode passivation using an organic small molecular of TCTA

Yu-Jie Hu¹, Zhi-Xiang Chen¹, Yi Xiang¹, Chuan-Hui Cheng^{1 *}, Weifeng Liu², and
Weishen Zhan¹

¹*School of Physics, Dalian University of Technology, Dalian 116024 China*

²*Mechanical and Electrical Engineering College, Hainan University, Haikou 570228
China*

*Corresponding author. Email: chengchuanhui@dlut.edu.cn

Experiment and Measurement

Sb₂Se₃ (99.999%) was purchased from Sigma. C₆₀, tris(8-hydroxyquinolino) aluminum (Alq₃), *N*, *N'*-bis(naphthalen-1-yl)-*N*, *N'*-bis-(phenyl)benzidine (NPB), and TCTA were sublimed grade and purchased from Han Feng. Solar cells were fabricated by the vacuum thermal evaporation with a base pressure of 2.0×10^{-4} Pa on commercially patterned ITO coated glass. The sheet resistance of the ITO film is $\sim 10 \Omega \text{ cm}^{-2}$. Substrates were ultrasonically washed in soapsuds, deionized water, acetone, alcohol, and deionized water in sequence, and then dried by a flow of nitrogen gas. Substrates were subsequently baked in air at 200 °C for 20 min. Next, TCTA and Sb₂Se₃ were successively deposited on the ITO at room temperature by the vacuum thermal evaporation. Then, the vacuum was broken and substrates were transferred to a vacuum tube furnace with two temperature zones to anneal at 280 °C for 30 min in the atmosphere of Se, and was naturally cooled down to room temperature. During the annealing process the source of Se was kept at 210 °C, and a mixture of the argon and hydrogen gas (10:1 in volume, 99.999%) was admitted to flow into the tube at 30 sccm through a mass flow controller. The pressure in the tube was kept at ~ 35 Pa. After that, C₆₀ and Alq₃ were successively deposited by the vacuum thermal evaporation. Finally, substrates were transferred to another chamber without breaking the vacuum, in which

aluminum electrode was deposited by the vacuum thermal evaporation. A stainless shadow mask was used to define the device profile ($1.5 \times 5.0 \text{ mm}^2$). The film thickness was monitored by the quartz crystal microbalance. The deposition rates were $\sim 0.1 \text{ nm s}^{-1}$ for the TCTA, Sb_2Se_3 , C_{60} and Alq_3 , and $\sim 2.0 \text{ nm s}^{-1}$ for the Al electrode.

Absorption spectra were measured on a Shimadzu UV3600 spectrophotometer. X-ray diffractions (XRD) were performed on a Bruker D8 Advance. Surface and cross-sectional images of the Sb_2Se_3 film were measured on a Bruker scanning electron microscopy (SEM). X-ray photoelectron spectroscopy (XPS) were measured on a Thermo escalab 250Xi. Current–voltage (J – V) characteristics were tested on a Keithley 2611A source meter. Photovoltaic responses were obtained under AM1.5 illumination from a Zolix Sirius-SS150A solar simulator (class AAA) at a power of 100 mW cm^{-2} . The illumination intensity on the cell was adjusted by a standard calibrated Si solar cell. External quantum efficiency (EQE) spectra were measured on a Zolix SCS100 analyzer. Capacitance and impedance measurements were performed on an UC2876 impedance analyzer in the darkness, where an alternating current (AC) voltage of 30 mV was applied. Transient photovoltage (TPV) was monitored by a Keysight DSOX3012T oscilloscope using a 532 nm nanosecond pulse laser (New Wave) as the pump source.

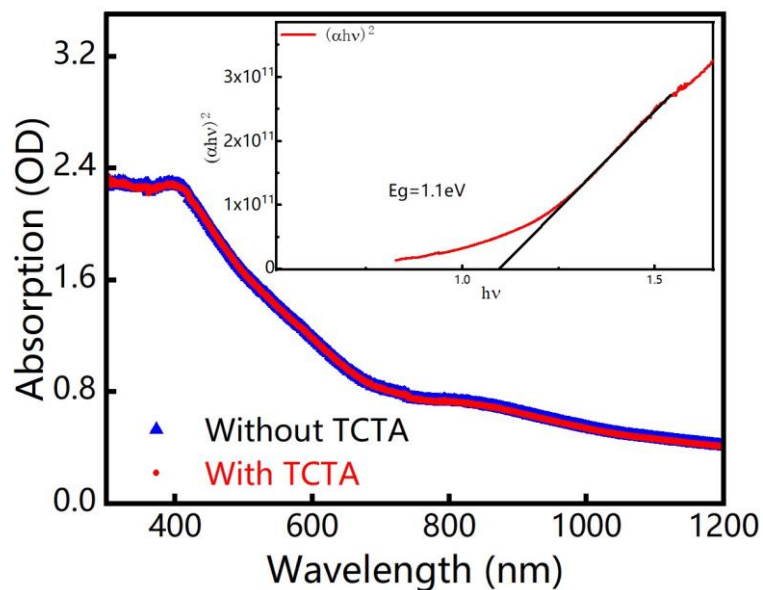


Fig. S1. Absorption spectra of the Sb_2Se_3 films (50 nm thick) on the glass with and without a TCTA buffer layer. A Tauc plot was given in the inset.

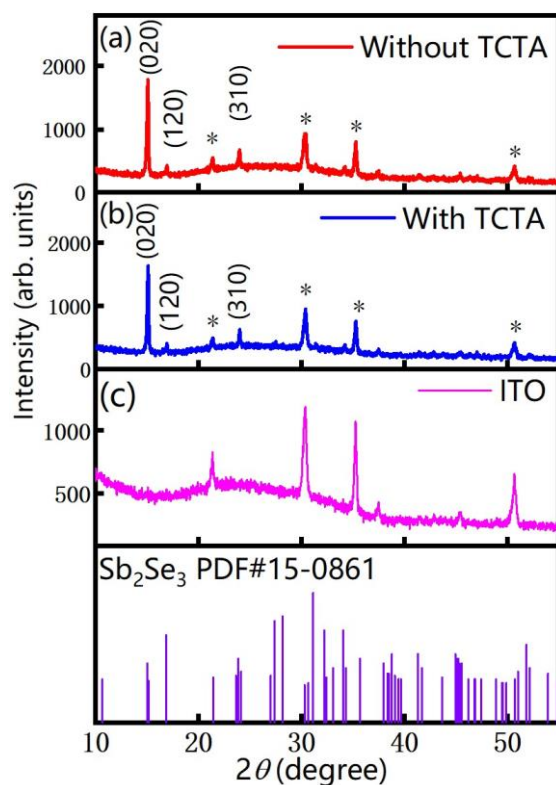


Fig. S2. XRD patterns of the Sb_2Se_3 films (150 nm thick) on the ITO with and without a TCTA layer. The pattern of the ITO substrate and the standard data of JCPDS 15-0861 are also given. The stars are the diffraction peaks of the ITO.

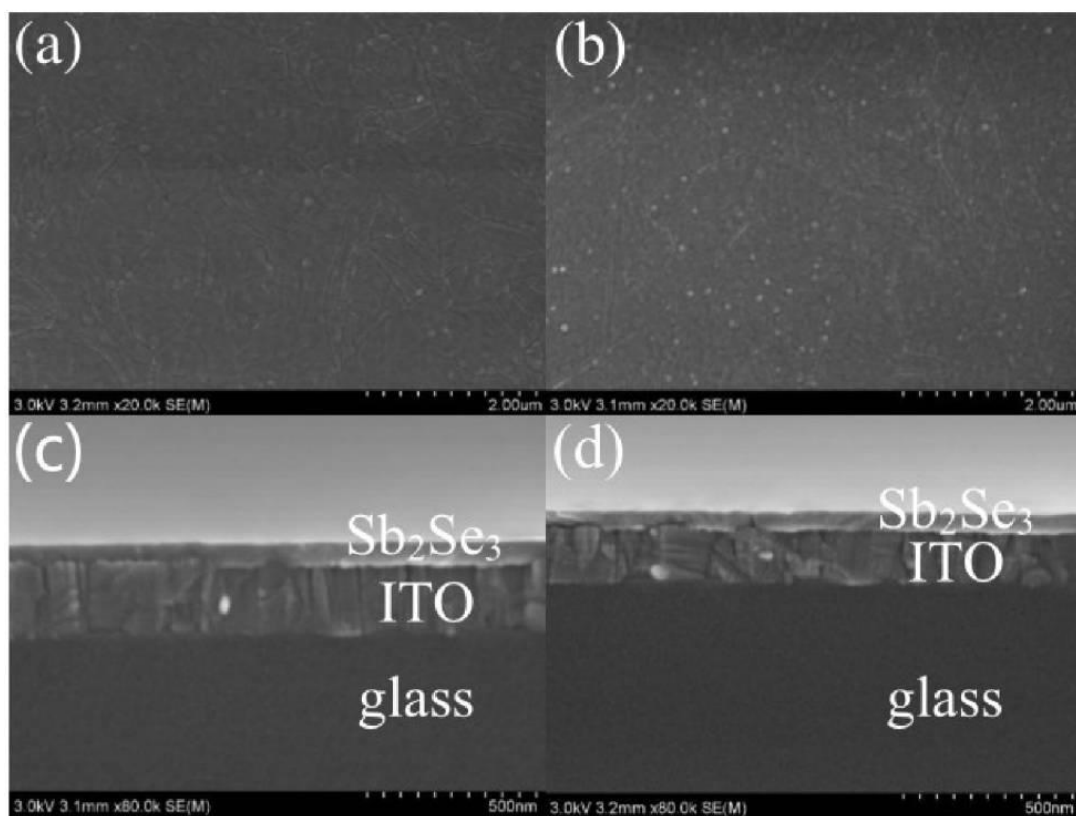


Fig. S3. Top-view SEM images of the Sb_2Se_3 films (a) without and (b) with a TCTA layer. The cross-sectional SEM images of the Sb_2Se_3 films (c) without and (d) with a TCTA layer.

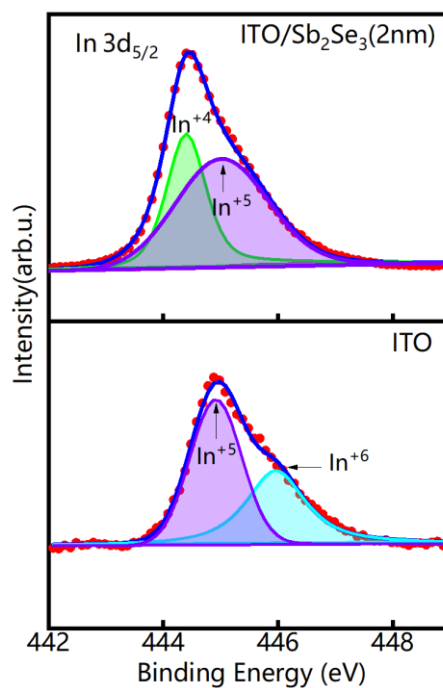


Fig. S4 XPS features of the $\text{In } 3d_{5/2}$. The red dots are the experimental data, and the blue lines are the fit results.

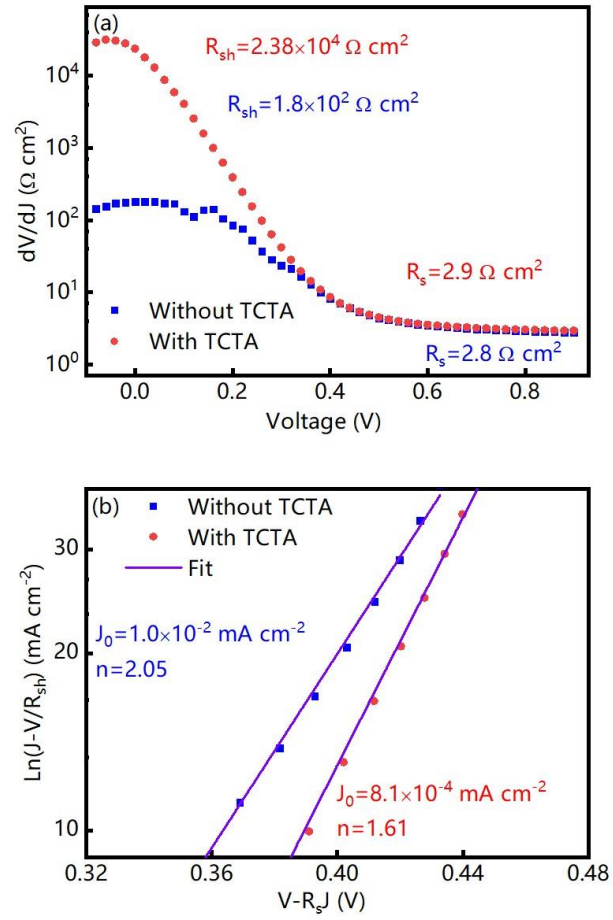


Fig. S5. The plots of (a) dV/dJ vs. V and (b) $\ln(J-V/R_{sh})$ vs. $(V-JR_s)$, which are extracted from the $J-V$ characteristics in the darkness.

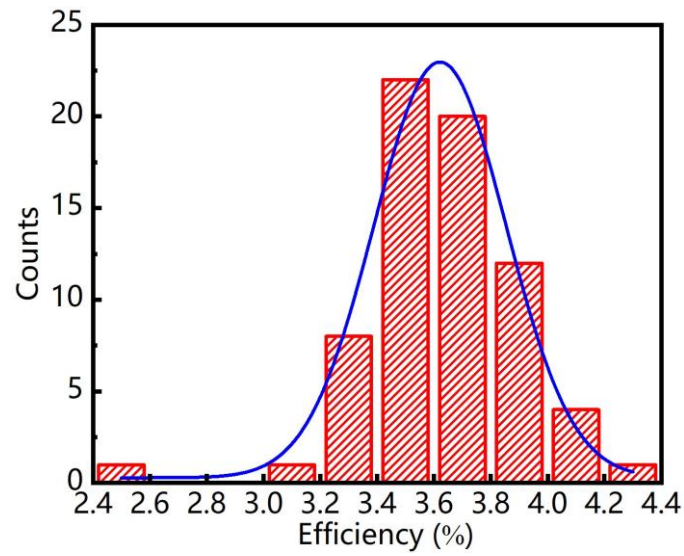


Fig. S6. Distribution of the PCEs of 69 solar cells. The blue line is the fit result.

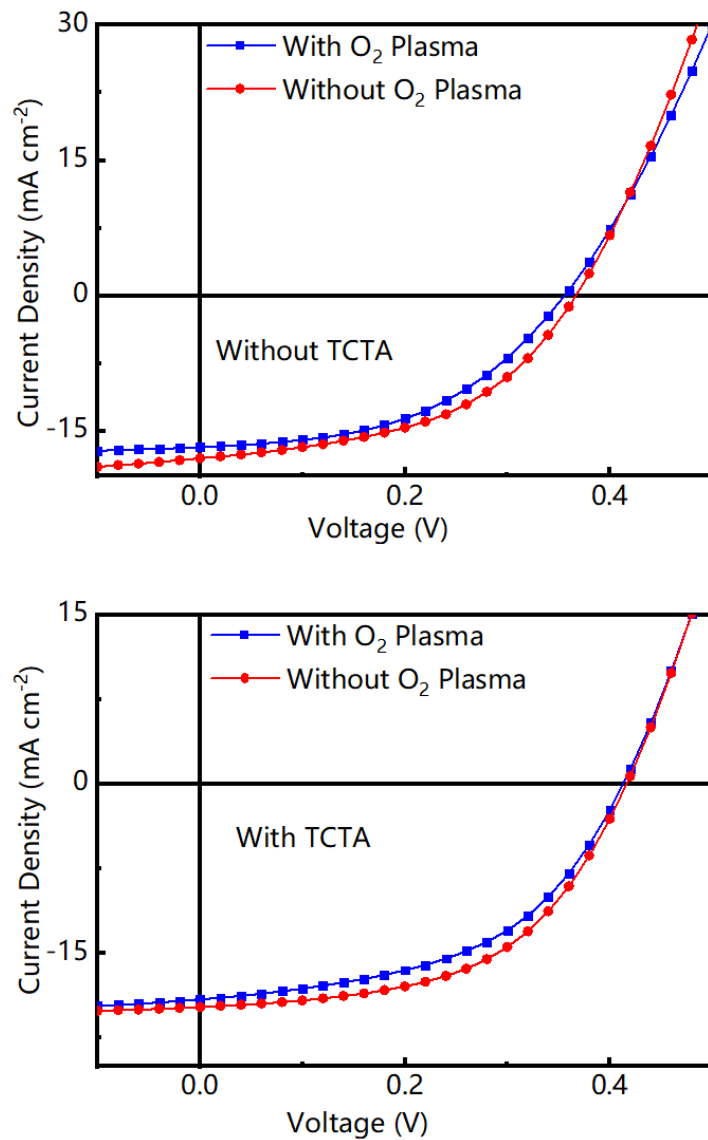


Fig. S7. J - V characteristics of the devices (b) with and (b) without an oxygen plasma treatment with and without a TCTA layer under one-sun illumination (AM 1.5 100 mW cm^{-2}).